

SAFETY IMPLICATIONS OF CLiFF LIQUID METAL FIRST WALLS^a

B. J. MERRILL¹, D.-K. SZE², H. Y. KHATER³, E. A. MOGAHED³

¹ INEEL Fusion Safety Program, P.O. Box 1625, Idaho Falls, ID, 83415-3860

² University of California, San Diego, CA

³ University of Wisconsin, Madison, WI

Abstract

In this article we explore some of the safety issues associated with the Advanced Power Extraction (APEX) liquid metal first wall (FW) concept called the Convective Liquid Flow First-Wall (CLiFF) design. In particular, we examine the chemical reactivity of and site boundary dose from three liquid metals being proposed for the CLiFF FW during a worst case confinement-boundary-bypass accident. The liquid metals considered are: lithium, tin, and gallium. The accident analyzed is a loss-of-vacuum accident (LOVA), during which air enters the CLiFF vacuum vessel (VV) from an adjoining room through a connecting diagnostic port or plasma heating duct. The resulting lithium fire was analyzed and the energy released from this fire was found to be manageable for the CLiFF blanket design presently under consideration. The estimated dose at the site boundary is less than the no-evacuation limit of 10 mSv for ground level releases if plant isolation occurs within several hours.

1. Introduction

The APEX study[1] was initiated in 1998 by the U.S. Fusion Energy Program with the primary objective of identifying and exploring novel chamber technology concepts that could substantially improve the attractiveness of fusion energy. A concept that has emerged from this study is a liquid metal FW concept called the CLiFF design. The idea behind CLiFF is to replace a solid FW with a fast flowing thin liquid metal film as the FW. This thin film provides a renewable liquid surface that is immune to radiation damage and surface erosion concerns, and

^a This work was prepared under the auspices of the US Department of Energy, Office of Fusion Energy Science, under the DOE Idaho Field Office contract number DE-AC07-99ID13727.

largely eliminates the thermal stress problems experienced by solid FW structures when exposed to very high surface heat fluxes.

In this article we explore some of the safety issues associated with the CLiFF design. In particular, we examine the chemical reactivity of, and site boundary dose from three liquid metals being proposed for the CLiFF FW during a worst case confinement-boundary-bypass accident. The three liquid metals being proposed for the CLiFF FW are: lithium, tin and gallium. At the present time, the CLiFF design team has adopted the SiC/LiPb blanket concept of the ARIES-AT design [2] as the CLiFF blanket. We have analyzed the response of this CLiFF design during a LOVA. We have chosen this accident because, based on previous safety studies [3], this accident produces significant environmental releases due to the fact that the primary radioactive confinement boundary of CLiFF, which is the CLiFF VV, could in theory fail. This occurs because a loss-of-offsite-power event results in a loss of plasma control and an induced plasma disruption. The induced plasma disruption in theory fails the windows of a diagnostic port or plasma-heating duct. As a consequence, air from a room adjoining the reactor enters the plasma chamber by way of the failed VV port. This air reacts with the high temperature metals inside of the CLiFF VV to release energy in the case of lithium, to mobilize radioactive material by oxidation, and to transport these mobilized materials to the environment by natural convection airflow through the failed VV port. Of ultimate concern regarding this accident is the risk this accident poses to the public. Under the DOE Fusion Safety Standard [4], the maximum allowable dose at the site should not exceed 10 mSv during worst case weather conditions. This dose limit insures that a site evacuation plan will not be required for the CLiFF facility.

We used the MELCOR code [5] to analyze the response of these CLiFF FW materials during this LOVA event. MELCOR is under continuing development at the Sandia National Laboratory (SNLA) to analyze severe accidents in fission reactors. MELCOR tracks the flow of two-phase water during such accidents, as well as any radioactive aerosols that may exist in either fluid phase. Structure temperatures are determined by one-dimensional heat conduction equation solutions. Heat transfer to both fluid phases is considered. External (walls) or internal (pipes) flow configurations are simulated during forced, natural, boiling, and condensation heat transfer modes. Modifications have been made to MELCOR at the INEEL for fusion specific analyses [6].

In the following sections we present the analyses performed to assess the safety issues for the liquid metals under consideration. Section 2 describes the LOVA calculation performed with MELCOR to determine the CLiFF VV pressurization rate and the magnitude of the VV bypass flow rate to the environment. Section 3 examines the chemical reaction issues associated with liquid lithium during this accident. Section 4 presents the models used to predict mobilization of FW radioactive material, the release of this material as aerosols to the environment, and the resulting site boundary dose from this release. Finally, conclusions are drawn in Section 5 based on the results presented in this paper.

2. LOVA calculation

To analyze this event, a MELCOR model of the CLiFF/ARIES-AT design [2] was developed. This model includes: 1) the free volume within the VV and pumping ducts, 2) the FW and VV wall components, 3) the confinement building upper functional rooms (UFR), 4) the ventilation system ducts of the UFR, 5) the walls of the UFR, and 6) a duct that connects the VV to the UFR. The free volume in the VV and pumping ducts was estimated to be 785 m³. The FW surface area is 425 m². The FW temperature history was taken from a two-dimensional ANSYS heat conduction code analysis of a loss-of-flow accident (LOFA) for the ARIES-AT solid wall APEX design [7], which is conservative because the LiPb decay heat for this design is about 30% more than that for this CLiFF design. The UFR has a combined volume of 5880 m³, and located at ground level elevation. The bypass duct that connects the VV to the UFR is assumed to have a cross-sectional area of 0.02 m² (diameter of 0.16 m), and a length of 10 m. The size of the duct has been selected to simulate a diagnostic port or a plasma-heating duct in the VV. The bypass duct was divided vertically into two flow paths to allow for the prediction of a counter-current flow pattern expected to develop within this duct during this event due to natural convection. The above UFR and bypass duct assumptions are those developed for the ITER EDA safety study [8].

Figure 1 contains the predicted VV pressure during this event. The pressure in the VV reaches atmospheric pressure by 200 seconds. Figure 2 contains the predicted flow in the bypass duct. The initial flow is choked flow into the VV at a rate of 3.4 kg/s, a flow condition that continues until about 70 seconds. Figure 2 shows that the flow in the duct becomes stratified

beyond 900 seconds at about 5 g/s. This flow drops to about 1 g/s after 24 hours as the internals of the CLiFF design cool.

3. Chemical reactions

Lithium is the only material of the three being considered as a CLiFF FW material that has significant chemical reaction issues. Lithium reacts vigorously with both air and water. During a LOVA, air enters the plasma chamber after the lithium has been heated to elevated temperatures by the energy released during the induced plasma disruption. In air, lithium reacts with oxygen to form lithium oxide and with nitrogen to form lithium nitride. Both of these lithium reactions are exothermic. The safety issue is not only the lithium fire that develops, but also whether or not enough energy will be released to fail in-vessel components.

To analyze this accident, a model was developed that describes the rate of surface heating from the lithium-air reaction, plus accounts for the two-dimensional effects of combined conduction and convection within a thin film. The oxidation equations for this model are similar to those adopted for the MELCOR code [9]. Here, the reaction rate is assumed to proceed as fast as oxygen or nitrogen can diffuse to the lithium surface through a gaseous boundary layer above the lithium surface. Because convective mass and heat transfer can be described by analogous boundary layer conservation equations [10], it has been determined that the surface boundary layer mass transfer coefficient (m/s) for the 'ith' specie (K_{mi}) can be related to surface boundary layer heat transfer coefficient through the following relationship [11]:

$$K_{mi} = Nu \left(\frac{D_i}{L} \right) \left(\frac{Sc}{Pr} \right)^{1/3} \quad (1)$$

where,

$$Nu = \text{Nusselt number} = \frac{h_a L}{k}$$

$$D_i = \text{mass diffusion coefficient (m}^2\text{/s)}$$

$$L = \text{characteristic length (m)}$$

$$Sc = \text{Schmidt number} = \frac{\mu}{\rho D}$$

$$\text{Pr} = \text{Prandtl number} = \frac{\mu c_p}{k}$$

and where h_a is the atmosphere heat transfer coefficient ($\text{W}/\text{m}^2\text{-K}$), k is the atmosphere thermal conductivity ($\text{W}/\text{m-K}$), μ is the atmosphere viscosity ($\text{kg}/\text{m}^2\text{-s}$), ρ is the atmosphere density (kg/m^3), and c_p is the atmosphere specific heat ($\text{J}/\text{kg-K}$).

The appropriate atmosphere heat transfer coefficient for this model was obtained from correlations for external natural and forced convection [12]. For forced convection, the atmosphere velocity was set equal to the film velocity that is initially 10 m/s. Given the mass transfer coefficient of Equation 1, the mass flux ($\text{kg}/\text{m}^2\text{-s}$) of oxygen arriving at the lithium surface is:

$$\Gamma_{\text{O}_2} = K_{\text{mO}_2} \rho_{\text{O}_2} \quad (2)$$

Equation 2 assumes that the oxygen is being consumed as fast as it arrives at the lithium surface. The energy liberated (W/m^2) by this reaction is given by

$$q_{\text{O}_2} = \Gamma_{\text{O}_2} H_{r_{\text{Li}_2\text{O}}} / (2 M_{\text{O}_2}) \quad (3)$$

where H_r is the heat of reaction for Li_2O ($\text{J}/\text{kg-mole}$), and M_{O_2} is the molecular weight of oxygen ($\text{kg}/\text{kg-mole}$). A relationship similar to Equation 3 was also derived for the lithium-nitrogen reaction that forms Li_3N .

The temperature of the lithium film is obtain by solving, in finite-difference form, the following energy equation written in the Cartesian co-ordinate system:

$$\rho c_p \left(\frac{\partial T}{\partial t} + u \frac{\partial T}{\partial x} \right) = \frac{\partial}{\partial x} \left(k \frac{\partial T}{\partial x} \right) + \frac{\partial}{\partial y} \left(k \frac{\partial T}{\partial y} \right) + q \quad (4)$$

where T is temperature (K), t is time (s), u is velocity (m/s) in the x-direction (m), and q represents bulk heating or imposed surface heating terms. The bulk heating for this model is that

due to either neutrons or decay heat. The imposed surface heat flux is due to either the plasma heat flux prior to the accident (2 MW/m^2), the disruption heat flux ($1.0 \times 10^5 \text{ MW/m}^2$ for a disruption time period of 1 ms), or the air oxidation heat flux of Equation 3. The poloidal distance (x-direction) a liquid metal FW is allowed to flow during normal operation is limited by allowable plasma impurity concentrations that result from FW surface evaporation. Unlike tin and gallium which can traverse the entire poloidal distance from the top to the bottom of reactor before exceeding their evaporation limits, lithium must be injected and extracted at four poloidal locations (every 3.5 m for the outboard FW) to avoid exceeding CLiFF plasma impurity limits. The total distance in the y-direction (or radial direction) for this model equals the FW film thickness of 2 cm, plus an additional 26 cm of the first blanket zone of the ARIES-AT blanket concept.

The ARIES-AT blanket concept is essentially a SiC tube within a SiC tube [2]. The annulus formed between the inner and outer tubes is 1 cm in width, and is the cooling channel for the outer tube (i.e., the blanket side walls). LiPb enters this channel at the bottom of the reactor, flows poloidally at a velocity of 4.3 m/s to the top of the reactor, makes a 180° turn, and flows poloidally down the inner tube at 0.11 m/s to exit the blanket at the bottom of the reactor. The inlet temperature for this design is 654°C . The LiPb coolant reaches an outlet temperature of 1100°C from the FW surface heat flux of 0.26 MW/m^2 and the neutron bulk heating of 0.91 MW/m^3 . We have tested our thermal model of this blanket for these heating conditions, with the velocities scaled by $1/4^{\text{th}}$ to obtain the correct ARIES-AT blanket temperature rise because our blanket module only covers $1/4^{\text{th}}$ of the outboard poloidal distance. The predicted average outlet temperature for this quarter-scale blanket is 1065°C , which is in fair agreement with the reported ARIES-AT design point. However, operating this scaled blanket at the ARIES-AT design temperatures would not be thermally efficient because a large quantity of high temperature heat would be lost to the much cooler 230°C lithium FW flow. As a consequence, for this scaled ARIES-AT blanket the inlet temperature was lowered to 400°C , which results in an outlet temperature of 710°C . Figure 3 contains the predicted operating temperatures of this blanket in the form of a 3D surface plot. During the LOVA the FW and blanket flow undergoes a flow coast down as a result of the complete loss of power (i.e., a complete station blackout). The rate of flow coast down was set at that prescribed in Reference [8].

The final modeling issue that must be addressed before this accident analysis can be completed is that regarding the transient behavior of the FW film. As a conservative assumption, we assume that the magnetically induced forces associated with the plasma disruption do not strip the liquid film from the blanket wall, and that the film will continue to drain until a minimum film thickness is achieved. Without experimental data to define what this minimum thickness is, an assumption regarding this thickness had to be made. While the film could be as thin as that of a wetting layer, it can not be thicker than a film that is unstable to Taylor density waves [13]. A liquid film that is unstable to these waves would breakup and form half-droplets on the substrate surface, with a circumference equal to or less than the critical Taylor wavelength. However, half-droplets of this size in a close pack array would only occupy 60% of the volume that a film would occupy. Therefore, the thickness of film that contains the mass equivalent to that of these droplets is given by

$$\delta_m \approx \left[\frac{\sigma}{g(\rho_f - \rho_g)} \right]^{1/2} \quad (5)$$

where σ is the liquid surface tension (N/m), and g is the gravitational constant (m/s^2). For lithium this film thickness is 8.3 mm, which is nearly 42% of the initial FW thickness.

Figure 4 contains the predicted maximum FW surface temperature and average FW film thickness as a function of time for a LOVA that starts at two seconds transient time. A maximum temperature of 2760 °C is reached during the disruption. At this temperature the energy losses due to surface evaporation and subsequent lithium vapor shielding nearly cancels the surface energy deposition coming from the plasma disruption. The film loses about 4 mm of thickness during the disruption, then drains to the critical film thickness of 8.3 mm within 200 ms. After the disruption, the surface temperature drops to near the lithium inlet temperature of 230 °C because insufficient air enters the VV by this time to sustain a significant lithium-air reaction. By 100 s, nearly atmospheric conditions are obtained within the VV (note Figure 1), and the oxidation reaction drives the lithium temperature to 1290 °C by 400 s. By this time the FW film burns away and the lithium fire extinguishes. Figure 5 is a surface plot of module temperatures after 400 s, illustrating that the LiPb, which is the only heat sink modeled for this accident, has risen in temperature as result of this fire.

Reference [14] claims that SiC could reach temperatures of 1500 °C without a significant loss of strength. Therefore, this accident should not fail the blanket walls. This suggests that no

LiPb will spill into the VV during this accident scenario, and that the radioactive Po-210 and Hg-203 inventories of the LiPb will not be mobilized within the facility. In addition, if the FW lithium nozzles and catch trays are made of SiC there should also be no mobilization of radioactive structural material during this accident. However given the severe nature of the predicted fire, if lithium were to be used as a CLiFF FW material the design options adopted for the EVOLVE concept [15] to inert rooms that connect to the VV should also be adopted for CLiFF.

4. Radioactive release

Because an online processing system will remove any implanted or bred tritium from a flowing FW, a lithium FW will contain negligible amounts of radioactivity. Also, the analysis of the previous section indicates that lithium fires can be tolerated by this APEX design without failing structural components and thereby releasing the blanket radioactive inventories. As a consequence, radioactive release calculations are not required for lithium as a FW material option for this accident scenario. However, tin and gallium first walls do have significant radioactivity release concerns. To illustrate this, for a given quantity of activated tin FW material released to the environment the specific dose is approximately 8 mSv/kg, based on radiological dose calculations^a provided by Reference 16 and APEX FW activation calculations provided by Reference 17. The top ten dose contributors are Sb-124, Sn-119m, Sb-123, Sb-122, In-114m, Sb-125, Sn-113, Sn-117m, Sn-121m, and Cd-113m. This specific dose suggests that 1.25 kg of tin could be released without exceeding the no-evacuation limit if one ignores preferential isotopic mobilization.

For most liquids, isotopic mobilization estimates can be made by modeling the liquid as an ideal solution^b and by making use of the kinetic theory for evaporation and condensation [18]. This gives the following mobilization rate ($\text{kg}/\text{m}^2\text{-s}$) for the 'ith' isotope:

^a Pasquill-Gifford stability class F plume conditions, wind velocity of 1 m/s, elevated 100 m release, and a site boundary of 1000 m.

^b The vapor pressure of an ideal solution follows Raoult's Law [19].

$$\Gamma_i = \left(\frac{M_i}{2\pi R} \right)^{1/2} \left[\frac{x_i p_{s,i}}{\sqrt{T_s}} - \frac{p_{g,i}}{\sqrt{T_g}} \right] \quad (6)$$

where:

R = Universal gas constant (J/kg-mole-K)

x_i = liquid mole fraction

$p_{s,i}$ = isotope material saturation pressure (Pa) at T_s

T_s = surface temperature (K)

$p_{g,i}$ = isotope material gas partial pressure (Pa)

T_g = gas temperature (K)

In order to determine the partial pressures of Equation 6, a transport calculation is required. To accomplish this calculation, a second kinetics equation similar to Equation 6 was solved to determine the rate of gas condensation onto or into aerosol particles. The solution of these two rate equations combined with a conservation of mass equation to predict gas density gives the required partial pressure of Equation 6 through the application of the ideal gas law. Once these gases condense onto or into aerosol particles, they are subsequently transported to the environment by way of the natural-convection-air-flow patterns described in Section 2.

With the use of Equation 6 and the saturation pressure curves contained in Figure 6, the impact that surface mobilization has on specific dose can be investigated. As can be seen in Figure 6, cadmium is the most volatile isotope in activated tin. Indium and antimony (once the temperature is above the antimony melting point of 630 °C) are two orders of magnitude less volatile than cadmium, but both materials are still two orders of magnitude more volatile than tin. If the vapor pressure curves of Figure 6, neglecting cadmium, are used in Equation 6 along with the assumption of zero gas partial pressure (i.e. $p_{g,i} = 0$), the resulting specific dose is 610 mSv/kg at 600 °C, with 98% of this dose due to In-114m. This dose is 75 times greater than the 8 mSv specific dose reported above because the more volatile isotopes are being preferentially mobilized in this more accurate modeling approach. While this is unwelcome news from a dose standpoint, it does bode well for the possibility of eliminating these isotopes from the FW stream by vapor separation methods. In fact, given the predicted production rates for the indium and antimony isotopes, the required efficiency of a system that could remove

these isotopes to levels at which the entire FW inventory could be released without exceeding the no-evacuation dose limit is only 4%, for a processing stream that is 0.1% of the FW flow [20]. By removing the cadmium, indium, and antimony isotopes, the specific dose for activated tin drops to approximately 3.7 mSv/kg.

When Equation 6 is applied to gallium, the top ten contributors to the specific dose are Zn-69m, Ga-72, Zn-69, Zn-71m, Ge-69, Ga-68, Ge-71, Ga-70, Cu-67, and Ni-65. The magnitude of the dose is 22 mSv/kg with 67% of the dose due to Zn-69m. However, the zinc isotopes are the most volatile isotopes in activated gallium. By removing zinc by an online vapor separation system, the specific dose for gallium drops to 5.4 mSv/kg.

The mobilization model described in this section was introduced into the MELCOR LOVA model described in Section 2 through a MELCOR user defined function subroutine. The total FW material inventory that could be mobilized during this accident equals that of the maximum film thickness as defined by Equation 5, which for liquid tin and gallium is approximately 3 mm. The time-dependent mobilization of tin and gallium for this LOVA is given in Figure 7. The entire FW film mass is mobilized within four hours for gallium and within twelve hours for tin. While more than 7000 kg of material has been mobilized during this accident, the amount released to the environment by way of the facility stack is less than a kilogram for both materials, as can be seen by the results presented in Figure 8. This represents a confinement factor (i.e., released mass divided by mobilized mass) for this accident of more than 11,000. Confinement of these materials is predicted to be this high because the environment within the VV is conducive to aerosol particle growth, producing a significant amount of settling before convection of these particles to the environment can occur. Because this is such a crucial result, a parameter study was conducted to determine how the mass released to the environment depends on initial film thickness. By running multiple cases with different initial film mass, it was determined that the confinement factor drops with decreasing initial film mass, for example an initial film mass of 100 kg results in a confinement factor of about 700. However, the mass released to the environment also decreases with initial film mass. Therefore, the release presented in Figure 8 is expected to be the maximum predicted release by our model for this accident.

The dose at the site boundary due to the release shown in Figure 8, if this release occurs by way of a 100 m high stack, is given in Figure 9. The results Figure 9 are very encouraging

because both materials meet the no-evacuation limit of 10 mSv. If a stacked release is not feasible, the resulting dose from a ground level release would be about a factor of ten higher. As a consequence, the facility would have to be isolated within 5.4 hours in the case of gallium, and 12 hours in the case of tin to insure that the no-evacuation limit is not exceeded for this bypass accident.

5. Conclusions

In this paper we have examined the safety concerns associated with three liquid metal candidates as flowing FW materials for the APEX CLiFF design. These safety concerns were addressed in the context of regulatory constraints enumerated in the DOE Fusion Safety Standard. During a worst case VV bypass accident, an accident which results in the failure of the primary radioactive confinement boundary of the CLiFF design, we determined that the lithium fire that would develop during this accident would not fail the SiC blanket structure presently being proposed for CLiFF. This indicates that for lithium as a FW material that little or no radioactive release would occur because the radioactive inventory of greatest concern is that in the LiPb blanket coolant. With regard to tin and gallium, we demonstrate that there will be a significant mobilization of radioactive material for this accident, and that only a fraction of this material will actually be carried to the environment by natural convection airflow currents. In addition, if online removal of the more volatile radioactive isotopes of these metals is performed and the release is stacked, the resulting dose at the site boundary will be less than the 10 mSv for which an evacuation plan would be required for the site. The general conclusion is that the three liquid metals presently under consideration for CLiFF can be made to be safe material options provided appropriate design constraints are adopted.

6. References

1. M. A. Abdou, "Exploring novel high power density concepts for attractive fusion systems," *Fusion Engineering and Design*, 45, 1999, pp. 145-167.
2. R. Raffray, et al., "Fusion power core engineering for the ARIES-AT power plant," to be published in *Fusion Engineering and Design*.

3. R. Aymar, et al., *Technical Basis for the ITER Final Design Report, Cost Reviews and Safety Analysis (FDR)*, ITER Design Team Document, S CA LS 39 97-12-19 F1, December 1997, pg. 4.3-5.
4. DOE STD 6003-96, *The Safety of Magnetic Fusion Facilities*, May 1996.
5. R. O. Gauntt, et al., *MELCOR Computer Code Reference Manuals: Version 1.8.4*, NUREG/CR-6619, Vol. 2, Rev. 1, July 1997, pp. HS-RM 37-41.
6. B. J. Merrill, R. L. Moore, S. T. Polkinghorne, D. A. Petti, "Modifications to the MELCOR code for application in fusion accident analysis," *Fusion Engineering and Design*, 51-52, 2000, pp. 555-563.
7. E. A. Mogahed, "LOCA/LOFA analysis for APEX LiPb/SiC solid wall concept in comparison to ARIES-AT," presentation at 2nd Electronic Meeting for FY 2001, <http://www.fusion.ucla.edu/APEX/>, August 9, 2001.
8. H.-W. Bartels, editor, "Accident Analysis Specifications for NSSR-2 (AAS)," version 2, S 81 RI 19 97-05-04 W1.1, SEHD 8.1.C-1, May 6, 1997.
9. B. J. Merrill, "A lithium-air reaction model for the MELCOR code for analyzing lithium fires in fusion reactors," *Fusion Engineering and Design*, Vol. 54, 2001, pp. 485-493.
10. J. R. Welty, C. E. Wicks, and R. E. Wilson, *Fundamentals of Momentum, Heat and Mass Transfer*, John Wiley & Sons, Inc., New York, 1969, pp. 534-558.
11. J. G. Collier, J. R. Thome, *Convective Boiling and Condensation*, 3rd edition, Clarendon Press, Oxford, 1994, pg. 442.
12. C. O. Bennett, J. E. Myers, *Momentum, Heat, and Mass Transfer*, 3rd ed., McGraw-Hill, New York, 1982, p. 375
13. G. I. Taylor, *Proceedings of the Royal Society, London*, Vol. A210, p.192, 1950.
14. W. Dienst, "Assessment of silicon carbide as potential wall protection material in fusion reactors," *Fusion Engineering and Design*, Vol. 16, p. 315, 1991
15. C. P. C. Wong, et al., "Evaluation of the tungsten alloy vaporizing lithium first wall and blanket concept," 14th Topical Meeting on the Technology of Fusion Energy, Park City, UT, Oct. 15-19, 2000.
16. M. L. Abbott letter to D. A. Petti, "Revised Results – MACCS2 Doses for Fusion Isotopes Release to the Atmosphere using P-G Dispersion Parameters," MLA-11-99, INEEL, April 14, 1999.

17. H. Y. Khater, "Activation Analysis of Sn," presentation at 2nd Regular Meeting for FY2000, <http://www.fusion.ucla.edu/APEX/>, November 15-17, 2001.
18. Collier, pg. 433.
19. G. J. Van Wylen, R. E. Sonntag, *Fundamentals of Classical Thermodynamics*, John Wiley and Sons, Inc., New York, 1965, pg. 486.
20. D. K. Sze, B. J. Merrill, H. Y. Khater, "Activation and Activation Product Control in Sn," presentation at 2nd Electronic Meeting for FY2001, <http://www.fusion.ucla.edu/APEX/>, August 9, 2001.

Figure Captions

Figure 1. Vacuum vessel pressure during a LOVA.

Figure 2. Bypass duct mass flow during a LOVA.

Figure 3. Initial temperature distribution of CLiFF blanket with lithium FW.

Figure 4. Lithium surface temperature and film thickness during a LOVA.

Figure 5. Temperature distribution of CLiFF blanket after the lithium fire caused by a LOVA.

Figure 6. Saturation vapor pressure of hazardous radioactive isotopes of activated tin.

Figure 7. CLiFF tin and gallium FW mobilized mass during a LOVA.

Figure 8. CLiFF tin and gallium FW mass released to environment during a LOVA.

Figure 9. Site boundary dose from tin and gallium release during a LOVA in CLiFF

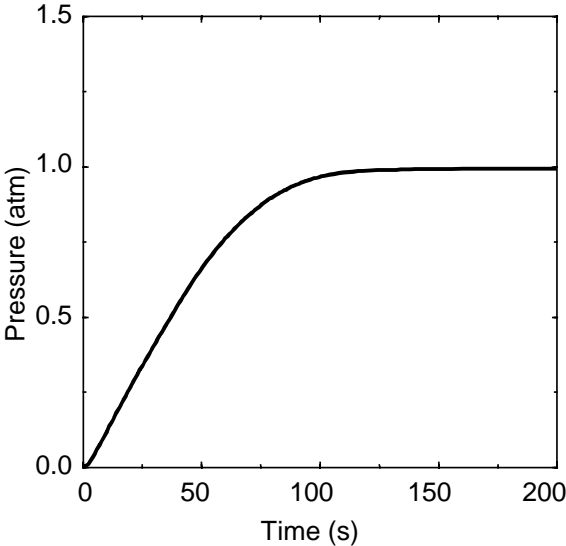


Fig. 1

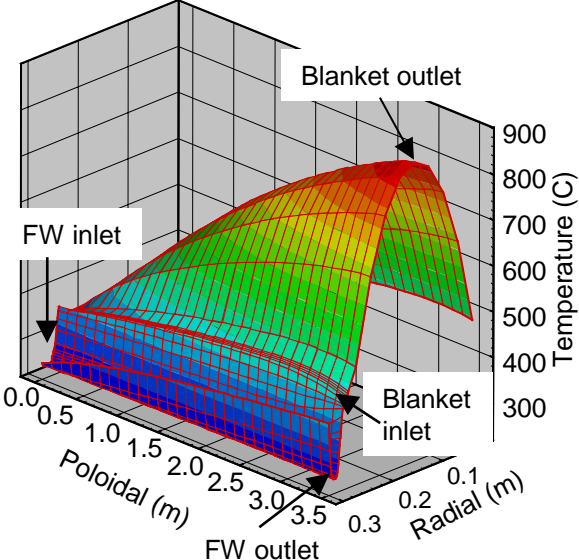


Fig. 3

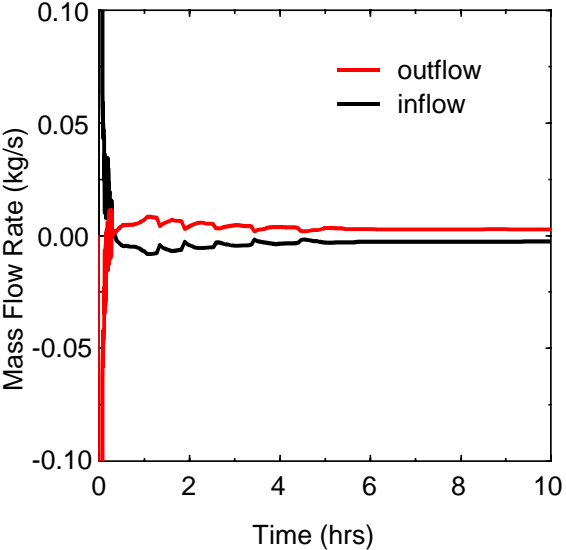


Fig. 2

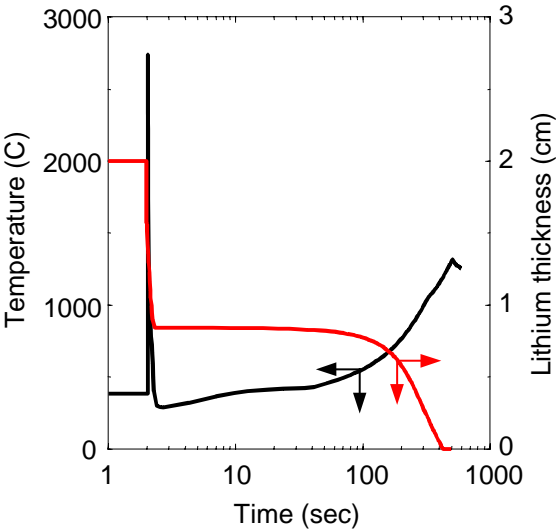


Fig. 4

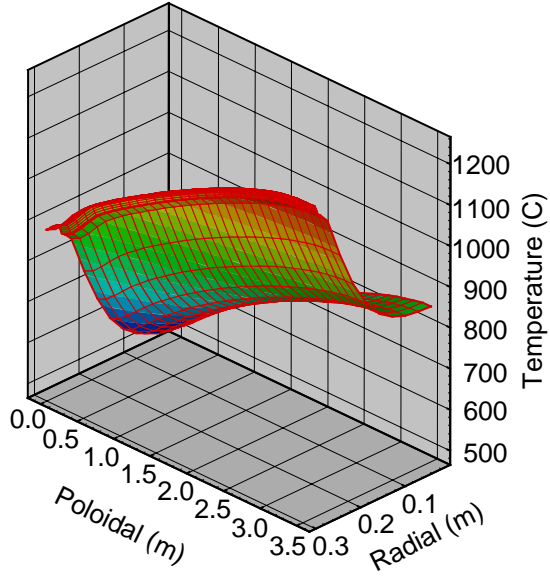


Fig. 5

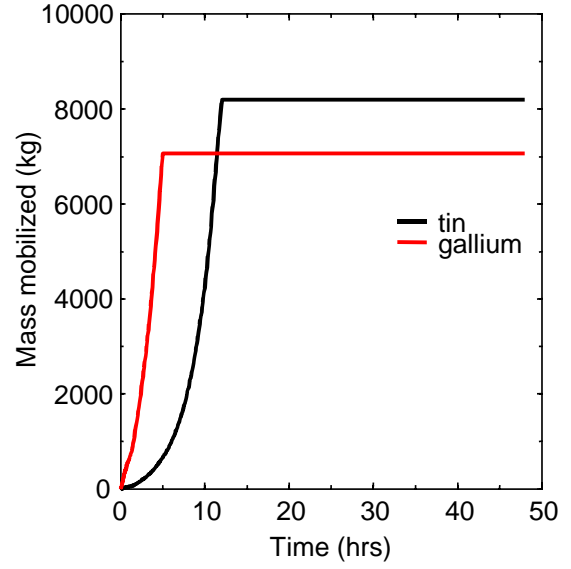


Fig. 7

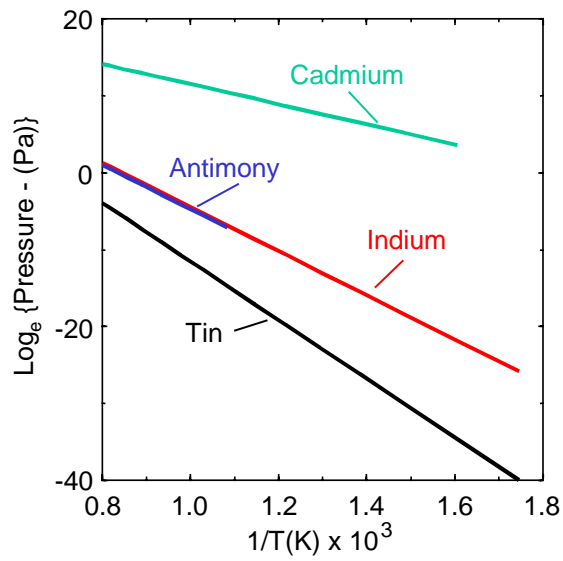


Fig. 6

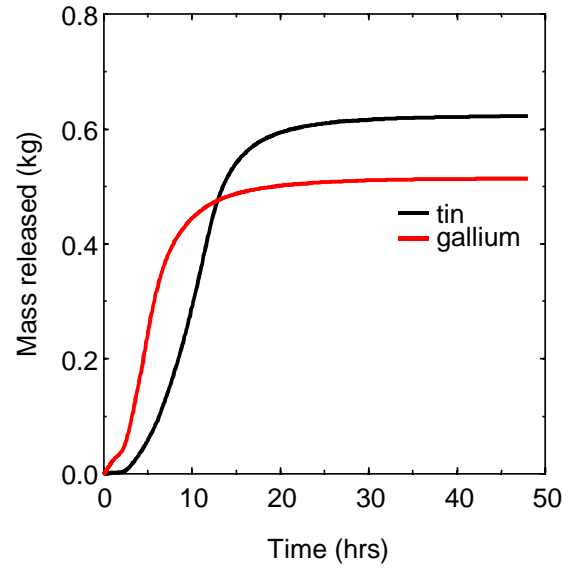


Fig. 8

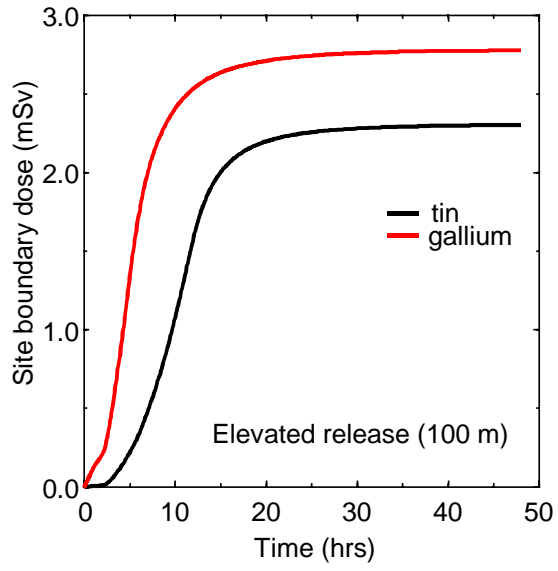


Fig. 9